Behavioral impulsivity is associated with pupillary alterations and hyperactivity in CDKL5 mutant mice

Viglione Aurelia[1$], Sagona Giulia[2$] Carrara Fabio[3], Amato Giuseppe[3], Totaro Valentino[1], Lupori Leonardo[2], Putignano Elena[4], Pizzorusso Tommaso[2,4], Mazziotti Raffaele[2,*]

1. BIO@SNS Lab, Scuola Normale Superiore via G. Moruzzi 1, 56124 Pisa, Italy
2. Department of Developmental Neuroscience, IRCCS Stella Maris Foundation, 56128 Pisa, Italy
3. ISTI – Istituto di Scienza e Tecnologia dell'Informazione, via G. Moruzzi 1, 56124 Pisa, Italy
4. Institute of Neuroscience, National Research Council, Via Moruzzi, 1 56124 Pisa, Italy

** Corresponding author: Raffaele Mazziotti, Istituto Neuroscienze CNR, Via G. Moruzzi,1 56125 Pisa ITALY, tel +390503153167, Fax +390503153220 e-mail: raffaele.mazziotti@in.cnr.it*

$ These authors contributed equally to this work

Abstract

Cdkl5 deficiency disorder (CDD) is a severe neurodevelopmental condition characterized by early-onset seizures in the first month of life, intellectual disability, motor and social impairment. No effective treatment is currently available and medical management is only symptomatic and supportive. Recently, mouse models of *Cdkl5* disorder have demonstrated that mice lacking *Cdkl5* exhibit autism-like phenotypes, hyperlocomotion, and dysregulations of the arousal system. In this study, we tested *Cdkl5* male and female mutant mice in an operant conditioning chamber to assess cognitive and motor abilities. The behavioral results show that CDD mice display impulsivity and hyperactivity together with low levels of cognitive flexibility and perseverative behaviors. Furthermore we assessed arousal levels by simultaneously recording pupil size and locomotor activity in basal conditions and in response to visual virtual reality. Pupillometry reveals in CDD mice a constitutively smaller pupil size and an impaired response to unexpected stimuli associated with hyperlocomotion, demonstrating a global defect in arousal modulation. Finally, machine learning reveals that both behavioral and pupillometry parameters can be

considered good predictors of CDD. Since early diagnosis is essential to evaluate treatment outcomes and pupillary measures can be performed easily, we proposed the monitoring of pupil size as a promising biomarker for CDD.

Keywords
CDKL5, CDD, Operant Conditioning, Pupillometry, Orienting Response, Pupillary Light Reflex

Introduction

Mutations in *cyclin-dependent kinase-like 5 (Cdkl5)*, an X-linked gene encoding for a serine-threonine kinase that is highly expressed in the forebrain (1), cause *Cdkl5* deficiency disorder (CDD). CDD is a severe neurological condition characterized by early-onset seizures in the first month of life, intellectual disability, motor and social impairment (EIEE2, OMIM number: #300672) (2,3). CDD has been genetically linked to multiple neurodevelopmental disorders, including Rett syndrome, early infantile epileptic encephalopathy and autism spectrum disorder (ASD) (4). In mice, *Cdkl5* is strongly upregulated postnatally, and seems to be active both in the cytoplasm and nucleus (5). *Cdkl5* was also found to be localized in postsynaptic structures, where it can regulate dendritic spine maturation and density, and modulate excitatory synaptic function (6,7). However, the role of *Cdkl5* in modulating neural substrates for cognitive and motor function is poorly understood and no effective treatment is currently available. Recent studies have demonstrated that mice lacking *Cdkl5* exhibit autism-like phenotypes, impulsivity and hyperlocomotion, resembling core symptoms of attention-deficit hyperactivity disorder (ADHD, OMIM 143465) (8). In addition, *Cdkl5* null mice present selectively elevated dopamine levels in the anterior forebrain, including the medial prefrontal cortex and the striatum, compared to wild-type (WT) mice (9). Deficits in attentional and executive functions in ADHD patients have been linked to dysregulations of the arousal system (10–12). Arousal alterations have also been reported in children with ASD and a recent study revealed arousal alterations in *Cdkl5*- and *MeCP2*-deficient mouse models (13). Here, we tested *Cdkl5* male and female mutant mice and their WT littermates in an operant conditioning (OC) chamber to assess cognitive and psychomotor abilities in an appetitive conditioning task, and we assessed arousal by simultaneous recording of pupil size and locomotor activity in basal conditions and in response to unexpected isoluminant stimuli presented in a virtual reality (VR) environment. The behavioral results indicated that CDD mice display an impulsive and hyperactive phenotype. Pupillometry showed decreased pupil size at rest associated with hyperlocomotion and an impaired orienting response to VR. These data reveal a global defect in arousal modulation in CDD mice, and introduce metrics for quantitative, non-invasive and translational biomarkers for neurodevelopmental disorders including CDD.

Results

Abnormal behavior of male and female *Cdkl5* mutant mice in an automated operant conditioning task.

In order to evaluate psychomotor and cognitive abilities in *Cdkl5* mice, we performed an appetitive conditioning task in *Cdkl5* (P60) null mice (*Cdkl5*$^{-/y}$) and WT littermates control (*Cdkl5*$^{+/y}$), using a 3D printed and automated operant conditioning chamber (Fig.1 A) (14). Operant conditioning (15) is a standard technique used in experimental psychology in which animals, including rodents (16,17), learn to perform an action to achieve a reward. Using this paradigm makes it possible to extract learning curves, accurately measure mental chronometry [e.g., reaction times (RTs)], and track an animal's position to assess motor and spatial performances. During the task, the animal uses its position to trigger a new trial by remaining in a specific place (active area) for a given amount of time (1.5 sec). The visual stimulus consists of two bright blue dots, appearing above each response button. The mouse needs to touch one of the two buttons to obtain the reward. We found that *cdkl5*$^{-/y}$ mice produced an increasingly higher number of trials than *cdkl5+/y* mice, reaching a statistical difference on Day 3 (Fig. 1C). *Cdkl5-/y* mice also showed reduced RTs (Fig.1 D) but no difference in intertrial intervals (time elapsing between the response and the activation of a novel trial, Fig.1 E). Moreover, the tracking analysis revealed altered locomotor activity in *cdkl5-/y* mice. In particular, during the task, *cdkl5-/y* mice moved faster and covered a greater distance than *cdkl5+/y* (Supplementary Fig.1).

Most CDD patients are heterozygous females carrying missense, nonsense, splice, or frameshift *Cdkl5* gene mutations or a genomic deletion (18). In females, the phenotypic spectrum of the disease spans from mild to severe forms, while boys carrying mutations in *Cdkl5* have more severe epileptic encephalopathy than girls (19,20). Thus, we decided to test *Cdkl5* heterozygous female mice (*cdkl5+/-*). Again, we found that *cdkl5+/-* mice performed a higher number of trials than control littermates (*cdkl5+/+*) (Fig.1 F). In particular, we found a statistical difference in the number of trials performed, already present on Day 1 and Day 2 (Fig.1 F). *Cdkl5+/-* mice also showed reduced RTs (Fig.1 G) and intertrial intervals compared to *cdkl5+/+* (Fig.1 H). Thus, *cdkl5+/-* mice are also altered in this behavioural task.

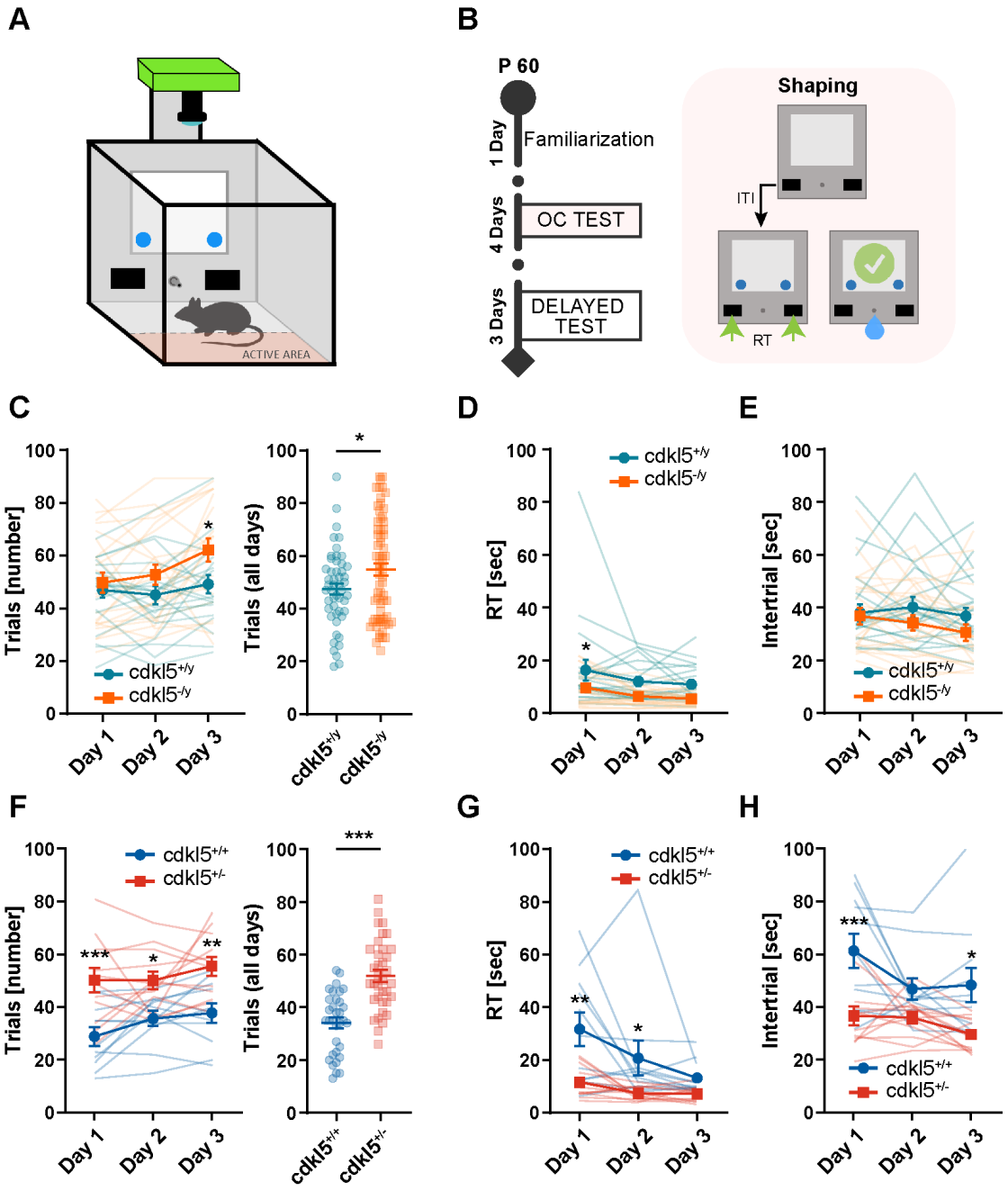

Figure 1: Shaping results in *Cdkl5* male and female mice. [A] Schematic representation of the conditioning chamber; **[B]** Diagram showing the appetitive conditioning timeline and the shaping paradigm; **[C]** On the left, single day trials in male mice: two-way ANOVA, effect of time < 0.05, effect of genotype < 0.05; post hoc Sidak multiple comparisons at Day 3 < 0.05. On the right, number of trials performed in the three days of shaping: P-value < 0.05, Unpaired T-Test; **[D]** Reaction Time in male mice: two-way ANOVA, effect of time < 0.005, effect of genotype < 0.005; post hoc Sidak multiple comparisons at Day 1 < 0.05; **[E]** Intertrial intervals in male mice show no differences between genotypes; **[F]** On the left, single day trials in female mice: two-way ANOVA, effect of genotype < 0.001; post hoc Sidak multiple comparisons at Day 1 < 0.001, Day 2 < 0.05, Day 3 < 0.01. On the right, number of trials performed in the three days of shaping: P-value < 0.0001, Unpaired T-Test; **[G]** Reaction Time [RT] in female mice: two-way ANOVA, effect of time < 0.05, effect of genotype < 0.05; post hoc Sidak multiple comparisons at Day 1 < 0.01, Day 2 < 0.05; **[H]** Intertrial

intervals in female mice: two-way ANOVA, effect of time < 0.05, effect of genotype < 0.01; post hoc Sidak multiple comparisons at Day 1 < 0.001, Day 3 < 0.05. n = 20 *cdkl5*$^{+/y}$; n = 22 *cdkl5*$^{-/y}$; n = 11 *cdkl5*$^{+/+}$; n = 12 *cdkl5*$^{+/-}$. *P-value < 0.05, **P-value < 0.01, ***P-value < 0.01. RT = Reaction Time; ITI = Intertrial.

Low level of cognitive flexibility, perseverative behavior, and hyperactivity in *Cdkl5* null mice

To better investigate the hyperactive behaviour observed in *cdkl5-/y* mice, we introduced a modified version of the operant task (Delayed Task, DT) (Fig.2 A). This test version increased the time needed to activate a single trial from 1.5 sec to 4 sec, thus requiring a stronger behavioural inhibition. The DT task revealed opposite results compared to the previous phase: *Cdkl5-/y* mice performed a lower average number of trials than *cdkl5+/y* littermates (Fig.2 B). In particular, we found a difference between groups in the number of trials performed on the first and second day of the DT (Day 5 and Day 6). This difference disappears on the last day of the test (Day 7) when *cdkl5-/y* mice reach the same performances as *cdkl5+/y* mice (Fig.2 B). We did not find differences in the RTs, demonstrating that the reduction in the number of trials was not attributable to a lack of interest in the task (Fig.2 C). However, we found a significant difference in the intertrial intervals. In particular, *cdkl5-/y* mice showed longer intertrial intervals in the first two days of the DT (Fig.2 D). These findings demonstrate lower cognitive flexibility of *cdkl5-/y* mice, probably due to an impairment in behavioural inhibition. We also introduced a new parameter called perseveration index (PI) to determine whether the learning impairment observed in *cdkl5-/y* mice was associated with perseverative and impulsive behaviours. In detail, PI counts every time the mouse follows the previous rule instead of the new one (e.g. waiting for 1.5 sec instead of 4 sec in the active area). We found a significantly higher PI in *cdkl5-/y* mice compared to *cdkl5+/y* on Day 5 and Day 6 (Fig.2 E). This suggests that for the first two days of the DT, *cdkl5-/y* mice continued to adopt the old operant task rules instead of adapting to the new paradigm, demonstrating an impairment in cognitive flexibility accompanied by impulsive and perseverative behaviours.

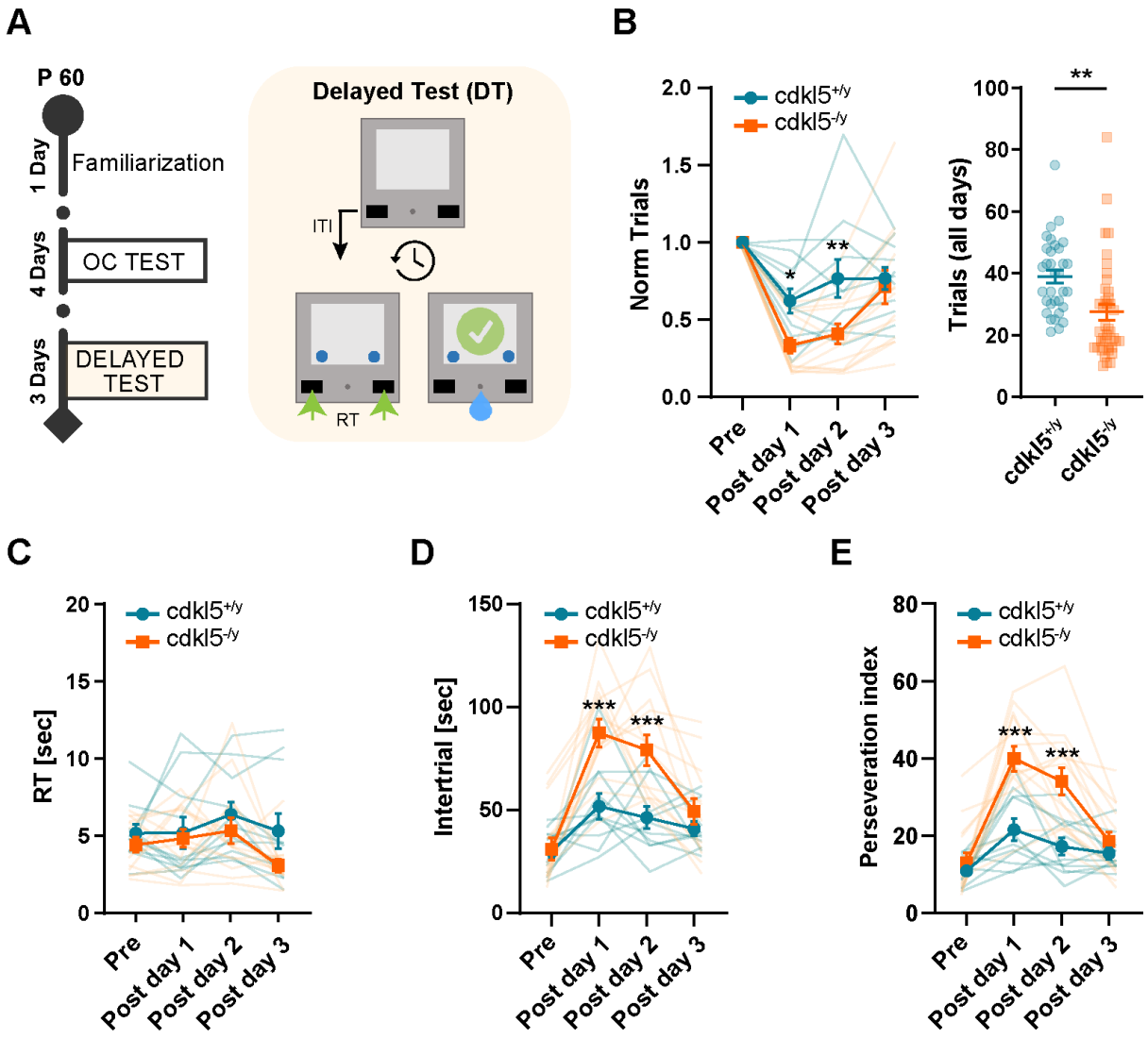

Figure 2: Delayed test in *Cdkl5* null mice. [A] Diagram showing the appetitive conditioning timeline and the DT paradigm; **[B]** On the left, trials normalized on the last day of the shaping phase (Day 4): two-way ANOVA, interaction time x genotype < 0.01, post hoc Sidak multiple comparisons at Day 5 < 0.05 and Day 6 < 0.01. On the right, number of trials performed in all the three day of DT: P-value < 0.01, Unpaired T-Test; **[C]** Reaction Time show no differences between genotypes; **[D]** Intertrial intervals: two-way ANOVA, interaction time x genotype < 0.01, post hoc Sidak multiple comparisons at Day 5 < 0.001 and Day 6 < 0.001; **[E]** Perseveration index: two-way ANOVA, interaction time x genotype < 0.001, post hoc Sidak multiple comparisons at Day 5 < 0.0001 and Day 6 = 0.0001. n = 11 *cdkl5*$^{+/y}$; n = 13 *cdkl5*$^{-/y}$. *P-value < 0.05, **P-value < 0.01, ***P-value < 0.01. RT= Reaction Time; ITI= Intertrial.

Head-fixed male and female *Cdkl5* mutant mice show an enhanced locomotor activity and a smaller pupil size

Spontaneous fluctuations in pupil size have been reported as a reliable index of arousal (21). Moreover, pupil function abnormalities have been described in children with attention deficits (e.g. ADHD) and ASD (22,23). We performed pupillometry in

P90 *cdkl5-/y* mice and *cdkl5+/y* littermates control (Fig.3 A). During pupillometry, mice were head-fixed and free to run on a circular treadmill equipped with an optical sensor to assess locomotor activity (Fig.3 B). Pupillometry was performed using MEYE Deep Learning tool (24). During pupillometry the animal was exposed to the following stimuli: a mean luminance uniform gray screen, a VR isoluminant stimulus composed of a virtual reality corridor moving coherently with the animal movement to elicit an orienting response (OR, Fig.3 B), and a high luminance white screen to assess the Pupillary Light Reflex (PLR). The uniform grey background was also presented before and after OR and PLR assessment to allow the pupil to return to baseline (Fig.3 B).

We first investigated pupil dynamics and locomotion in the absence of stimulation during the exposure to the uniform grey field. We found that *cdkl5-/y* mice exhibit enhanced locomotor activity (Fig.3 C) also in the head-fixed condition. In particular, *cdkl5-/y* mice showed more moving epochs and a higher velocity *per* epoch (Fig.3 D) than controls. We also found that the duration of a single running event was significantly longer in *cdkl5-/y* mice compared to *cdkl5+/y* (Fig.3 D). These results confirm in *cdkl5-/y* mice the hyperactive phenotype observed in the OC chamber, suggesting the presence of altered arousal levels. Pupillometric analysis revealed a constitutively smaller pupil size in *cdkl5-/y* mice compared to controls (Fig.3 E, D). However, the normalized pupil dilation induced by running was unaffected (Fig. S2).

Locomotor activity and pupil size were also affected in *cdkl5*+/- heterozygous female mice. In particular, locomotor activity was enhanced in *cdkl5*+/- mice as compared to control female *cdkl5*+/+, both in terms of time spent running and velocity (Fig.3 F, G). Moreover, as in male mutants, *cdkl5*+/- mice displayed a significantly smaller pupil size during running state and a strong trend ($p=0.057$) when resting (Fig.3 H).

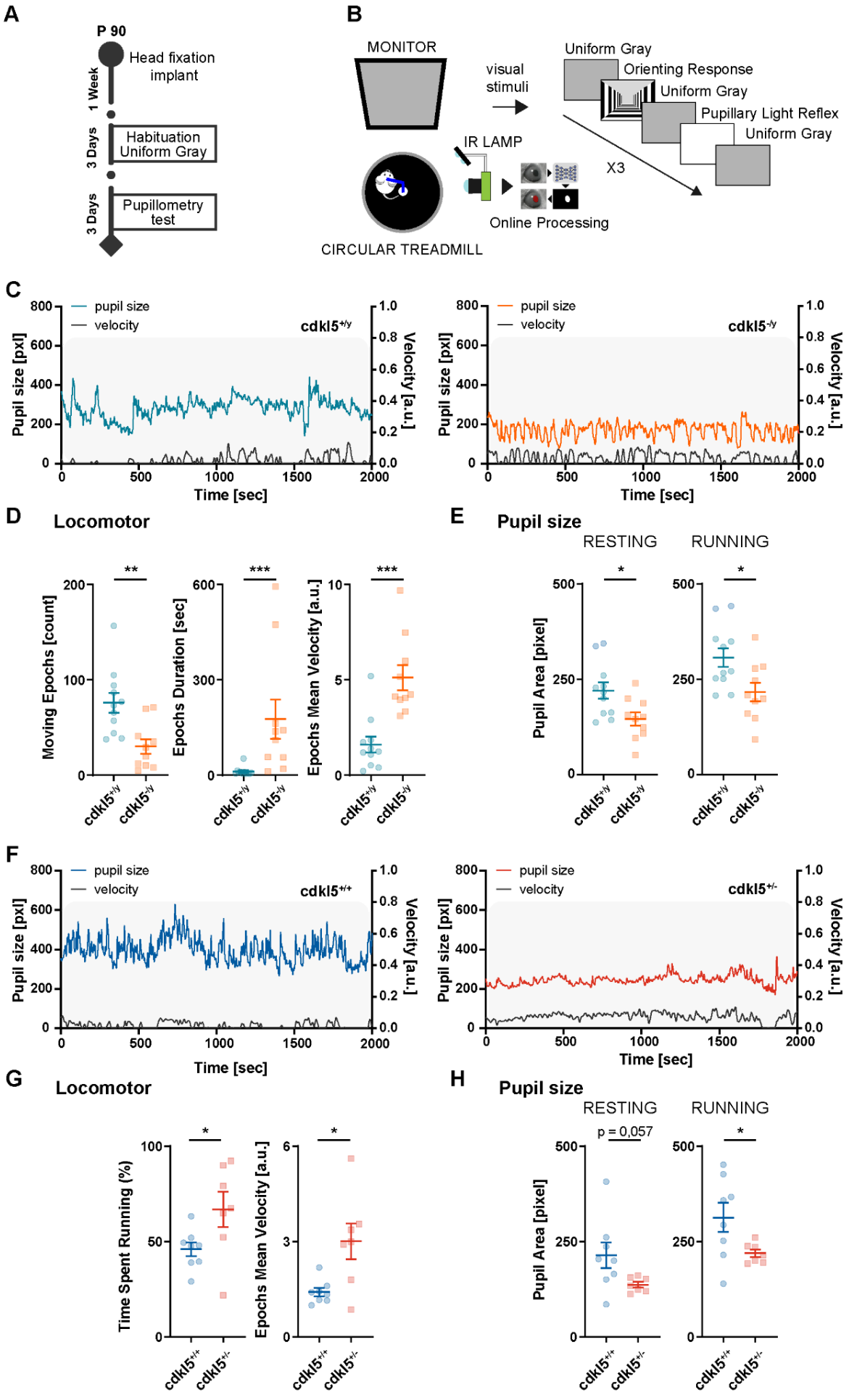
A
P 90
Head fixation implant
1 Week
3 Days
Habituation Uniform Gray
3 Days
Pupillometry test
B
MONITOR
visual stimuli
Uniform Gray
Orienting Response
Uniform Gray
Pupillary Light Reflex
Uniform Gray
X3
IR LAMP
Online Processing
CIRCULAR TREADMILL
C
pupil size
velocity
cdkl5+/y
cdkl5-/y
Pupil size [pxl]
Velocity [a.u.]
Time [sec]
D
Locomotor
Moving Epochs [count]
Epochs Duration [sec]
Epochs Mean Velocity [a.u.]
cdkl5+/y
cdkl5-/y
E
Pupil size
RESTING
RUNNING
Pupil Area [pixel]
F
cdkl5+/+
cdkl5+/-
G
Locomotor
Time Spent Running (%)
Epochs Mean Velocity [a.u.]
H
Pupil size
RESTING
RUNNING
p = 0,057
Pupil Area [pixel]

Figure 3: Locomotor activity and pupil size reveal arousal alterations in *Cdkl5* male and female mutant mice. **[A]** Diagram showing the pupillometry timeline; **[B]** Schematic representation of the head-fixed pupillometry setup. The mouse was head-fixed to a custom made metal arm equipped with a 3D printed circular treadmill to monitor running behavior. In the meantime, we assessed: baseline pupil size (uniform gray screen), OR (isoluminant VR) and the PLR (high luminance white screen). A single module was repeated three times. We repeated the same protocol on three different days; **[C]** Pupil diameter trace from a WT male mouse (*cdkl5*$^{+/y}$) and a *Cdkl5* null male mouse (*cdkl5*$^{-/y}$); **[D]** *Cdkl5* null mice showed an enhanced locomotor activity compared to WT, in terms of number of moving epochs (defined as a period of continuous movement), P-value < 0.01, Unpaired T-Test; moving epoch duration P-value < 0.05, Unpaired T-Test and epochs mean velocity, P-value < 0.001, Unpaired T-Test; **[E]** *Cdkl5*$^{-/y}$ showed a constitutively smaller pupil size compared to cdkl5$^{+/y}$ both during resting and running (resting, P-value < 0.05; running, P-value < 0.05; Unpaired T-Test); **[F]** Pupil diameter trace from a WT female mouse (*cdkl5*$^{+/+}$) and a *cdkl5* heterozygous female mouse (*cdkl5*$^{+/-}$); **[G]** *cdkl5*$^{+/-}$ mice showed an enhanced locomotor activity compared to *cdkl5*$^{+/+}$, in terms of percentage of time spent running, P-value < 0.05, Unpaired T-Test and velocity, P-value < 0.05, Unpaired T-Test; **[H]** *cdkl5*$^{+/-}$ mice showed a baseline smaller pupil size compared to *cdkl5*$^{+/+}$ during running, P-value < 0.05, Unpaired T-Test, and a strong trend in resting, P-value = 0.057, Unpaired T-Test. n = 11 *cdkl5*$^{+/y}$, n = 10 *cdkl5*$^{-/y}$; n = 8 *cdkl5*$^{+/+}$, n = 7 *cdkl5*$^{+/-}$. *P-value < 0.05, **P-value < 0.01, ***P-value < 0.01.

Cdkl5 null mice show altered orienting response but intact pupillary light response

The OR is an automatic and immediate response to an unexpected stimulus or changes in the environment (25–27) with effects on different levels of body responses (i.e., motor system, autonomic nervous system, and central nervous system) (25,27,28) including changes in pupil size and locomotion (29). Automatic OR to unexpected changes in the environment is a prerequisite for adaptive behaviour; it is perceived as a disruption of the current attentional focus to immediately respond to changes in the environment on a physiological, behavioural, and cognitive level. Previous studies have demonstrated atypical visuospatial orienting response in children with attention-related deficits and ASD (22,30,31). Thus, we investigated the OR induced by the VR stimulus.*cdkl5y/-* mice clearly showed an OR consisting of a substantial pupil dilation immediately after the stimulus onset. By contrast, *cdkl5y/-* mice displayed a dramatically reduced and transient pupillary response (Fig.4 A). VR also induced different locomotor responses. In particular, while VR elicited an increase in motility of *cdkl5y/+* mice, *cdkl5y/-* mice did not show significant changes in running velocity (Fig.4 B). Finally, we tested whether PLR, an autonomic reflex that constricts the pupil in response to an increase in luminance, was changed in *Cdkl5* mutants. As shown in Fig.4 C, we did not observe any significant differences in pupil constriction amplitude (maximal relative change in pupil area during constriction) or pupil re-dilation (maximal relative change in pupil area to recover the constriction). These results reveal an unaltered

PLR, suggesting a central origin for the OR alterations observed. Taken together, these results demonstrate in *cdkl5y/-* mice an altered physiological and behavioural response to an orienting visual stimulus.

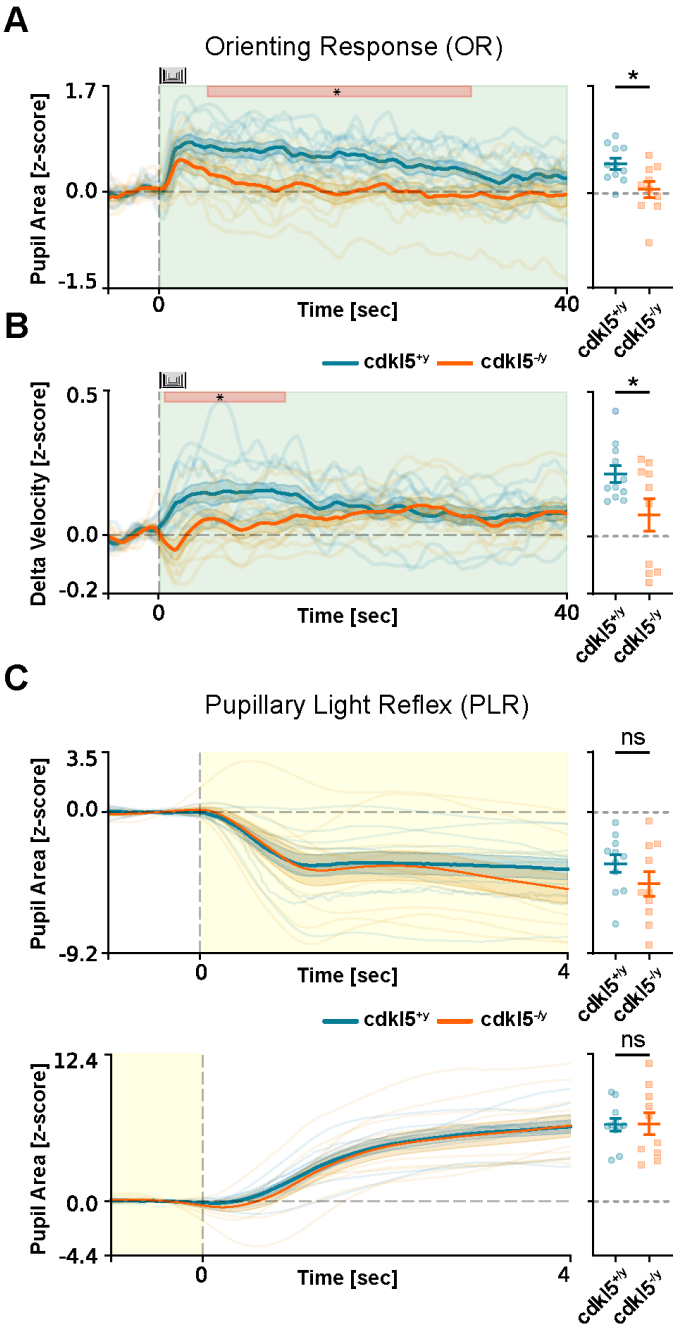

Figure 4: Pupillary OR and PLR assessment . [A] On the left, the average fluctuation of pupil size for all the stimulus repetitions. On the right the average pupil size. During the presentation of the orienting stimulus, *cdkl5*$^{y/-}$ mice showed a reduced pupillary dilation compared to *cdkl5*$^{y/+}$ (P-value < 0.05, Unpaired T-Test); shaded area represents the presentation of the VR stimulus **[B]** On the left, the average running velocity for all the stimulus repetitions. On the right the average velocity. *Cdkl5*$^{y/-}$ mice showed a different behavioral response compared to *cdkl5*$^{y/+}$ (P-value < 0.05, Unpaired T-Test), shaded area represents the presentation of the VR stimulus; **[C]** PLR response reveals no significant differences in both pupil constriction (top) and pupil re-dilation (bottom) between *cdkl5*$^{y/-}$ mice and

cdkl5$^{y/+}$. On the left, single animal traces and average fluctuation (thick line) of pupil size. Shaded area represents the presentation of the high luminance stimulus. Vertical dashed lines represent the onset of the visual stimulus. On the right the average pupil size during pupil constriction and pupil re-dilation. and . n = 11 *cdkl5*$^{+/y}$, n = 10 *cdkl5*$^{-/y}$. *P-value < 0.05, ns = not significant.

Behavioral appetitive conditioning parameters and head-fixed pupillometric and behavioral responses are robust predictors of *Cdkl5* null mice alterations

To test whether the behavioral and pupillary alterations observed in *Cdkl5* null mice can be used to classify single animals, we employed machine learning algorithms to build models capable of predicting mouse genotype from the behavioral and pupillary alterations that we measured. We found that by training the models only with the behavioral parameters collected during the OC task, almost all the models showed a remarkable discriminative capability between mutated and WT mice. In particular, depending on the model adopted, single mouse accuracy ranged between 77 and 83% and sensitivity between 75 and 87% (Table 1). The same machine learning models were employed to test the predictive power of the alterations found in *Cdkl5* mutant mice during pupillometry. Interestingly, we found that the pupillary and behavioral responses collected during the pupillometric assessments were good genotype predictors, with accuracy between 77 and 83% and sensitivity between 79 and 83% (Table 2). Finally, when we combined in the models the OC parameters with the parameters acquired during pupillometry, we found that the prediction power remarkably increased, reaching an accuracy between 77 and 91% and sensitivity between 73 and 91% (Table 3).

Table 1. Genotype classification of machine learning algorithms using OC parameters

Model	Accuracy (Mean %)	Specificity (Mean %)	Sensitivity (Mean %)	Permutation Scores (%)	p-value	Significance
SVC	82.8	88.4	78.6	52.5	< 0.01	**
MLP Classifier	82.5	80.0	86.8	53.1	< 0.01	**
Gaussian Process Classifier	81.9	85.2	83.2	52.8	< 0.01	**
Decision Tree Classifier	81.3	84.3	81.0	51.0	< 0.01	**
AdaBoost Classifier	81.2	83.9	83.0	51.6	0.02	*
Logistic Regression	76.9	80.3	75.25	53.3	< 0.01	**
K Neighbors Classifier	74.2	84.8	66.3	52.9	0.12	**ns**
Dummy Classifier	50.4	51.2	48.4	50.1	0.47	**ns**

Abbreviations: OC, Operant Conditioning; ns, not significant.

Table 2. Genotype classification of machine learning algorithms using head-fixed recorded parameters

Model	Accuracy (Mean %)	Specificity (Mean %)	Sensitivity (Mean %)	Permutation Scores (%)	p-value	Significance
Logistic Regression	83.1	86.1	82.5	52.3	0.02	*
MLP Classifier	81.7	82.9	83.1	51.2	0.02	*
SVC	81.0	82.2	80.9	49.9	<0.01	**
Ada Boost Classifier	80.1	87.7	74.3	50.0	0.02	*
Decision Tree Classifier	79.7	85.7	73.1	50.3	<0.01	**
Gaussian Process Classifier	77.1	79.4	79.7	50.4	0.02	*
K Neighbors Classifier	73.7	74.8	74.7	49.2	0.11	**ns**
Dummy Classifier	48.8	47.3	49.9	50.6	0.18	**ns**

Abbreviations: OR, Orienting Response; ns, not significant.

Table 3. Genotype classification of machine learning algorithms using OC and head-fixed recorded parameters

Model	Accuracy (Mean %)	Specificity (Mean %)	Sensitivity (Mean %)	Permutation Scores (%)	p-value	Significance
MLP Classifier	91.4	92.6	91.7	51.1	0.02	*
Logistic Regression	88.8	89.6	88.3	50.8	0.04	*
SVC	87.7	92.9	84.4	50.6	< 0.01	**
Gaussian Process Classifier	86.6	93.6	81.0	50.4	< 0.01	**
K Neighbors Classifier	82.4	94.5	70.5	51.2	< 0.01	**
Decision Tree Classifier	78.8	86.1	72.6	50.8	< 0.01	**
Ada Boost Classifier	77.2	82.8	73.7	51.2	< 0.01	**
Dummy Classifier	51.5	50.8	52.5	49.2	0.62	**ns**

Abbreviations: OC, Operant Conditioning; OR, Orienting Response; ns, not significant.

Discussion

This study reported alterations in behavioural and physiological parameters of male *Cdkl5* deficient and female heterozygous mice capable of classifying CDD mice with high accuracy and sensitivity. Behavioural impairment was assessed in an OC task using a fully automated and standardized operant conditioning chamber (14). In agreement with previous studies, (8,9), the OC task revealed hyperactive and impulsive behaviour in both male and female Cdkl5 mutant mice. We also demonstrated lower levels of cognitive flexibility, linked to an impairment in behavioural inhibition in *cdkl5* null mice. Indeed, while mutant mice could successfully perform more trials than controls if they had to wait only for a short time, they persevered with the previous strategy if the waiting time was prolonged, resulting in less successful trials than controls. Intriguingly, symptoms of inattention and hyperactivity, features of ADHD, have been frequently documented in children with ASD (32) and could also be present in CDD patients, although the CDKL5 gene has not been linked to ADHD in a genome-wide association study (33). Previous studies showed that impulsivity and hyperlocomotion of Cdkl5 null mice could be corrected by methylphenidate, an inhibitor of the dopamine transporter clinically effective in improving ADHD symptoms, suggesting a role for dopaminergic impairment in mediating impulsivity deficits (8,9). Our study shows that the presence of hyperactivity is also associated with impairment in processes controlling general arousal in Cdkl5 mice assessed measuring pupil size regulation and locomotor behaviour. We found that Cdkl5 mutants stay longer than wild-type mice in a high arousal state characterized by a dilated pupil and running. Absolute values of pupil size were always significantly smaller than controls in both male null and female heterozygous Cdkl5 mutant mice, although relative pupillary dilation during running or pupillary response to illumination change was unaffected. Constitutive smaller pupil size is reported to be linked with working memory and cognitive abilities and could be linked to altered activity of the locus coeruleus-noradrenergic system (34–36). Our study also revealed alterations in pupillary response to unexpected visual stimuli, a component of the OR commonly used also for human assessment(29). Indeed, we found that while wild-type mice exhibited a considerable and sustained pupil dilation in response to unexpected stimuli while mutants showed a smaller and transient dilation. Correspondingly, the presentation of the unexpected stimulus led to an increased running in wild-type mice but not in mutant mice. Overall, these data are consistent with a scenario in which Cdkl5 mutants are most of the time in a high arousal state that is not further increased by novel stimuli. Notably, the PLR analysis did not show alterations, demonstrating that the observed pupillary alterations are attributable to central dysfunctions rather than iris muscle or autonomic control abnormalities. The central

origin of these deficits is in line with a recent study by Artoni et al. revealing broadly distributed pupil sizes as a signature shared by mouse models of idiopathic or monogenic ASD, comprising CDD (13). In particular, in this study, the pupillary deficit of MeCP2 deficient mice could be rescued by the selective expression of MeCP2 in cholinergic circuits. The neural underpinnings underlying the deficits observed by our study is still to be explored. CDKL5 mRNA is expressed in cholinergic nuclei and superior colliculus (mousebrain.org), two structures implicated in central pupillary control and OR (29,37). However, in-depth investigation is needed to clarify this point.

Our machine learning models revealed that behavioural impulsivity and OR assessed by pupillometry are good predictors of CDD, with an enhanced power when evaluated together. Pupillometry is a non-invasive, quantitative and fully translational tool already used in clinical practice that requires minimal collaboration by the subject, and it has been used even in newborns and preterm infants at postpartum age of 1 day (38). Recently developed methods are opening the possibility to perform these measurements in a clinical and a domestic environment (24). Since early diagnosis is essential to evaluate treatment outcomes and pupillary measures can be performed quickly, also in preverbal subjects, we propose the monitoring of resting state and OR pupillometry as a promising and practical biomarker for CDD.

Materials and Methods

Animal handling

Animals were maintained in rooms at 22°C with a standard 12-h light-dark cycle. During the light phase a constant illumination below 40 lux from fluorescent lamps was maintained. Food (standard diet, 4RF25 GLP Certificate, Mucedola) and water were available ad libitum and changed weekly. Open-top cages with wooden dust free bedding were used. All the experiments were carried out according to the directives of the European Community Council (2011/63/EU) and approved by the Italian Ministry of Health. All necessary efforts were made to minimize both stress and the number of animals used. The mice used in this work derive from the *Cdkl5* null strain in C57BL/6N background developed in (39), and backcrossed in C57BL/6J for seven generations. Male WT mice were bred with female heterozygous to obtain mutant and WT littermates. Weaning was performed at postnatal day (P)21–23. Genotyping (P10–12) was performed on tail tissue as described in (39). We tested mice from P60 to P120. Colony founders were selected for the absence of the rd8 retinal degeneration allele spontaneously present in

C57BL/6N mice (40). Data analysis was performed by experimenters blind to the genotype.

The Operant Conditioning protocol

To perform the appetitive conditioning task we used a custom made OC chamber, described in Mazziotti et al. 2020 (14). Before starting the experiments, mice were handled for one week 5 minutes per day. During OC protocol mice were water restricted (all mice maintained a body weight above 85% of their baseline). We performed a first day of familiarization, by placing each animal in the OC box for three sessions of 10 min, spaced by at least 2h between each other. During this phase, a liquid reward (1% saccharin), coupled with the reward tone (3300 Hz), is provided manually whenever the mouse is in the active area (located on the side opposite to the interface wall), in this way the animal learns where to find the reward and associate it with the tone. The day after the familiarization we start the OC task (3 sessions per day, duration: 4 days). In the OC phase a visual stimulus was introduced, consisting of two bright blue dots (luminance: 0.9 cd/m2, wavelength: 465–475 nm, diameter: 5 mm) that appear above the two buttons after waiting for 1.5 sec in the activation area. Mice must touch one of the two buttons to obtain the liquid reward. We quantify the number of trials per session, the reaction time [RT] (the time between the activation of the trial and the button touch), the intertrial interval [ITI] (the time elapsed between the response and the activation of a new trial), the speed and distance travelled. A second group of mice, after the OC task, was introduced to the DT (duration 3 days). In this new version of the test the time needed to activate a new trial was extended from 1.5 sec to 4 sec. In order to evaluate the ability to inhibit a learned automatic response, we also introduced the perseveration index using a custom made Matlab software processing the mouse tracking data. To analyze mouse tracking data the arena is virtually divided into 256 (16×16) bins and raw exploration is z-scored to obtain relative exploration measures. In particular, a perseveration was counted every time the mouse exited the active zone before the 4 sec limit.

Surgery

Mice were deeply anesthetized using isoflurane (3% induction, 1.5% maintenance), placed on a stereotaxic frame and head fixed using ear bars. Prilocaine was used as a local anesthetic for the acoustic meatus. Body temperature was maintained at 37 degrees using a heating pad, monitored by a rectal probe. The eyes were treated with a dexamethasone-based ophthalmic ointment (Tobradex, Alcon Novartis) to prevent cataract formation and keep the cornea moist. Respiration rate and response to toe pinch were checked periodically to maintain an optimal level of

anesthesia. A subcutaneous injection of Lidocaine (2%) was performed prior to scalp removal. The Skull surface was carefully cleaned and dried, and a thin layer of cyanoacrylate was poured over the exposed skull to attach a custom-made head post that was composed of a 3D printed base equipped with a glued set screw (12 mm long, M4 thread, Thorlabs: SS4MS12). The implant was secured to the skull using cyanoacrylate and UV curing dental cement (Fill Dent, Bludental). At the end of the surgical procedure, the mice recovered in a heated cage. After 1 hour, mice were returned to their home cage. Paracetamol was used in the water as antalgic therapy for three days. We waited for seven days before performing head-fixed pupillometry to provide sufficient time for the animals to recover.

Pupillometry

During pupillometry, mice were head-fixed and free to run on a circular treadmill. We employed a modified version of the apparatus proposed by Silasi et al. (41), equipped with a 3D printed circular treadmill (diameter: 18cm). Velocity was detected using an optical mouse below the circular treadmill. To record the pupil, we used a USB camera (oCam-5CRO-U, Withrobot Lens: M12 25mm) connected to a Jetson AGX Xavier Developer Kit (NVIDIA) running a custom Python3 script (30fps). Real-time pupillometry was performed using MEYE (24), a convolutional neural network that performs online pupillometry in mice and humans (24). Before the experiments, mice were handled for one week 5 minutes each day; then, they were introduced gradually to head-fixation for an increasing amount of time for three days (habituation). During Day 1 and 2, we performed two sessions of 10 minutes of head-fixation, one in the morning and one in the afternoon. On Day 3, we performed one session of twenty minutes. During each head-fixation session, a curved monitor (24 inches Samsung, CF390) was placed in front of the animal (at a distance of 13 cm), showing a uniform grey with a mean luminance of 8.5 cd/m2. After the habituation phase, we performed the pupillary assessments. The assessment contains different epochs:

1) Uniform grey with a mean luminance (225 sec of a uniform grey screen, mean luminance of 8.5 cd/m2). Sixty minutes of a grey background is presented for 60 seconds between each epoch.

2) VR coherent with the animal movement eliciting an orienting response (180 sec). Composed of a luminance linearized procedural virtual corridor written in C# and running in Unity. The virtual corridor was composed of sine-wave gratings at different orientations (walls at 0° and floor at 90°) and spatial frequencies (from 0.06 to 0.1 cycles/deg), with a mean luminance of 8.5 cd/m2. The animal position in the virtual corridor was updated using an optical mouse connected to the circular treadmill.

3) PLR (15sec white screen. Luminance: 30 cd/m2).

Each epoch is presented three times for a total duration of 30 minutes.
For the pupillary assessment of female mice we evaluated baseline pupil size and locomotion during the presentation of a uniform grey screen with a mean luminance of 8.5 cd/m2.

Machine Learning

Machine learning models were fitted and evaluated using Python and Scikit-Learn.
All adopted models are binary classifiers predicting the genotype from numeric behavioural and physiological features. We considered as behavioural parameters, the number of trials per session, the RT and the ITI during the OC test and DT; as physiological features we condidered the average pupil size in resting and in ranning, the running speed, the running duration, and the pupillary ratio between resting and running in the different visual presentations.
Input features are standardised before training. The specific models we adopt, together with the hyperparameter we tuned, are the following. The default Scikit-Learn parameters are used where not specified.

A. Logistic Regression with L2 regularization (42); regularization strength is searched in logarithmic scale in $[10^{-4}, 10^{5}]$.
B. Support Vector Machine Classifier (SVC, (43)); we test linear and gaussian kernels; the regularization parameter and the kernel scaling coefficient (only for gaussian kernels) are searched in logarithmic scale respectively in $[10^{-4}, 10^{5}]$ and $[2^{-4}, 2^{5}]$.
C. Gaussian Process Classifier (44) with unitary RBF kernel.
D. Decision Tree (45) with maximum depth searched in [1, 6].
E. AdaBoost Classifier (46) with a 1-level-deep decision tree as base estimator.
F. K-Nearest Neighbors Classifier with uniform neighbors weighting; the best number of neighbors k is searched in [1,3].
G. Multi-layer Perceptron (MLP) Classifier (47) with one 100-neuron hidden layer and ReLU activation; the network is trained with the Adam optimizer for 1000 iterations; the learning rate and L2 regularization strength parameters are grid-searched respectively in [0.001, 0.01, 0.1] and [0.0001, 0.01, 1, 10].

For each model and each configuration of hyperparameters, the mean and standard deviation of accuracy, specificity, and sensitivity are computed using 100 bootstrapped data splits; in addition, a permutation test with 100 permutation is performed using the 5-fold accuracy as score. For brevity, only the best-performing configuration of hyperparameters is reported for each model. As a baseline, we also report the performance of the random classifier (Dummy Classifier).

Data analysis and statistics

Data analysis was performed using Python (Pupillometry and locomotion activity) and Matlab (Operant conditioning). Resting and running epochs are identified using an automated algorithm written in Python. The beginning of a moving epoch is defined as a period of at least 2 seconds in which velocity is higher than 1% with respect to the peak velocity of the subject. The epoch ends when velocity is below 1% for at least two seconds.
The statistical analysis was performed using Python custom scripts and GraphPad Prism 7.

Authors' contributions

RM, GA and TP designed the research; AV, EP, and GS performed the experiments, RM, GS, AV, LL, VT, FC and TP performed data analysis.

Acknowledgments

We gratefully acknowledge NVIDIA Corporation's support with the Jetson AGX Xavier Developer Kit's donation for this research.

Funding

This work was partially supported by AIRETT Associazione Italiana per la sindrome di Rett Project "Validation of pupillometry as a biomarker for Rett syndrome and related disorders: longitudinal assessment and relationship with disease"; Orphan Disease Center University of Pennsylvania grant MDBR-19-103-CDKL5; Associazione "CDKL5 - Insieme verso la cura"; and AI4Media - A European Excellence Centre for Media, Society and Democracy (EC, H2020 n. 951911) .

Competing interests

The authors declare that they have no competing interests.

References

1. Montini, E., Andolfi, G., Caruso, A., Buchner, G., Walpole, S.M., Mariani, M., Consalez, G., Trump, D., Ballabio, A. and Franco, B. (1998) Identification and Characterization of a Novel Serine– Threonine Kinase Gene from the Xp22 Region. *Genomics*, **51**, 427–433.
2. Moseley, B.D., Dhamija, R., Wirrell, E.C. and Nickels, K.C. (2012) Historic, clinical, and prognostic features of epileptic encephalopathies caused by CDKL5 mutations. *Pediatr. Neurol.*, **46**, 101–105.
3. Weaving, L.S., Christodoulou, J., Williamson, S.L., Friend, K.L., McKenzie, O.L.D., Archer, H., Evans, J., Clarke, A., Pelka, G.J., Tam, P.P.L., *et al.* (2004) Mutations of CDKL5 cause a severe neurodevelopmental disorder with infantile spasms and mental

retardation. *Am. J. Hum. Genet.*, **75**, 1079–1093.
4. Wang, I.-T.J., Allen, M., Goffin, D., Zhu, X., Fairless, A.H., Brodkin, E.S., Siegel, S.J., Marsh, E.D., Blendy, J.A. and Zhou, Z. (2012) Loss of CDKL5 disrupts kinome profile and event-related potentials leading to autistic-like phenotypes in mice. *Proc. Natl. Acad. Sci. U. S. A.*, **109**, 21516–21521.
5. Rusconi, L., Salvatoni, L., Giudici, L., Bertani, I., Kilstrup-Nielsen, C., Broccoli, V. and Landsberger, N. (2008) CDKL5 expression is modulated during neuronal development and its subcellular distribution is tightly regulated by the C-terminal tail. *J. Biol. Chem.*, **283**, 30101–30111.
6. Ricciardi, S., Ungaro, F., Hambrock, M., Rademacher, N., Stefanelli, G., Brambilla, D., Sessa, A., Magagnotti, C., Bachi, A., Giarda, E., *et al.* (2012) CDKL5 ensures excitatory synapse stability by reinforcing NGL-1–PSD95 interaction in the postsynaptic compartment and is impaired in patient iPSC-derived neurons. *Nature Cell Biology*, **14**, 911–923.
7. Della Sala, G., Putignano, E., Chelini, G., Melani, R., Calcagno, E., Michele Ratto, G., Amendola, E., Gross, C.T., Giustetto, M. and Pizzorusso, T. (2016) Dendritic Spine Instability in a Mouse Model of CDKL5 Disorder Is Rescued by Insulin-like Growth Factor 1. *Biol. Psychiatry*, **80**, 302–311.
8. Jhang, C.-L., Huang, T.-N., Hsueh, Y.-P. and Liao, W. (2017) Mice lacking cyclin-dependent kinase-like 5 manifest autistic and ADHD-like behaviors. *Hum. Mol. Genet.*, **26**, 3922–3934.
9. Jhang, C.-L., Lee, H.-Y., Chen, J.-C. and Liao, W. (2020) Dopaminergic loss of cyclin-dependent kinase-like 5 recapitulates methylphenidate-remediable hyperlocomotion in mouse model of CDKL5 deficiency disorder. *Hum. Mol. Genet.*, **29**, 2408–2419.
10. Strauß, M., Ulke, C., Paucke, M., Huang, J., Mauche, N., Sander, C., Stark, T. and Hegerl, U. (2018) Brain arousal regulation in adults with attention-deficit/hyperactivity disorder (ADHD). *Psychiatry Res.*, **261**, 102–108.
11. Geissler, J., Romanos, M., Hegerl, U. and Hensch, T. (2014) Hyperactivity and sensation seeking as autoregulatory attempts to stabilize brain arousal in ADHD and mania? *Atten. Defic. Hyperact. Disord.*, **6**, 159–173.
12. Martella, D., Aldunate, N., Fuentes, L.J. and Sánchez-Pérez, N. (2020) Arousal and Executive Alterations in Attention Deficit Hyperactivity Disorder (ADHD). *Front. Psychol.*, **11**, 1991.
13. Artoni, P., Piffer, A., Vinci, V., LeBlanc, J., Nelson, C.A., Hensch, T.K. and Fagiolini, M. (2020) Deep learning of spontaneous arousal fluctuations detects early cholinergic defects across neurodevelopmental mouse models and patients. *Proc. Natl. Acad. Sci. U. S. A.*, **117**, 23298–23303.
14. Mazziotti, R., Sagona, G., Lupori, L., Martini, V. and Pizzorusso, T. (2020) 3D Printable Device for Automated Operant Conditioning in the Mouse. *eNeuro*, **7**.
15. Jones, F.N. (1939) The behavior of organisms: an experimental analysis. .
16. Francis, N.A. and Kanold, P.O. (2017) Automated Operant Conditioning in the Mouse Home Cage. *Front. Neural Circuits*, **11**, 10.
17. O'Leary, J.D., O'Leary, O.F., Cryan, J.F. and Nolan, Y.M. (2018) A low-cost touchscreen operant chamber using a Raspberry Pi^{TM}. *Behav. Res. Methods*, **50**, 2523–2530.
18. Bahi-Buisson, N., Villeneuve, N., Caietta, E., Jacquette, A., Maurey, H., Matthijs, G., Van Esch, H., Delahaye, A., Moncla, A., Milh, M., *et al.* (2012) Recurrent mutations in the CDKL5 gene: genotype-phenotype relationships. *Am. J. Med. Genet. A*, **158A**, 1612–1619.
19. Liang, J.-S., Huang, H., Wang, J.-S. and Lu, J.-F. (2019) Phenotypic manifestations

between male and female children with CDKL5 mutations. *Brain Dev.*, **41**, 783–789.
20. Kluckova, D., Kolnikova, M., Medova, V., Bognar, C., Foltan, T., Svecova, L., Gnip, A., Kadasi, L., Soltysova, A. and Ficek, A. (2021) Clinical manifestation of CDKL5 deficiency disorder and identified mutations in a cohort of Slovak patients. *Epilepsy Res.*, **176**, 106699.
21. Joshi, S., Li, Y., Kalwani, R.M. and Gold, J.I. (2016) Relationships between Pupil Diameter and Neuronal Activity in the Locus Coeruleus, Colliculi, and Cingulate Cortex. *Neuron*, **89**, 221–234.
22. Boxhoorn, S., Bast, N., Supèr, H., Polzer, L., Cholemkery, H. and Freitag, C.M. (2020) Pupil dilation during visuospatial orienting differentiates between autism spectrum disorder and attention-deficit/hyperactivity disorder. *J. Child Psychol. Psychiatry*, **61**, 614–624.
23. Wainstein, G., Rojas-Líbano, D., Crossley, N.A., Carrasco, X., Aboitiz, F. and Ossandón, T. (2017) Pupil Size Tracks Attentional Performance In Attention-Deficit/Hyperactivity Disorder. *Scientific Reports*, **7**.
24. Mazziotti, R., Carrara, F., Viglione, A., Lupori, L., Lo Verde, L., Benedetto, A., Ricci, G., Sagona, G., Amato, G. and Pizzorusso, T. (2021) MEYE: Web App for Translational and Real-Time Pupillometry. *eneuro*, **8**, ENEURO.0122–21.2021.
25. Sokolov, E.N. (1963) Higher nervous functions; the orienting reflex. *Annu. Rev. Physiol.*, **25**, 545–580.
26. Sokolov, E.N. (1990) The orienting response, and future directions of its development. *Pavlov. J. Biol. Sci.*, **25**, 142–150.
27. Lynn, R. (2013) Attention, Arousal and the Orientation Reaction: International Series of Monographs in Experimental Psychology. *Attention, Arousal and the Orientation Reaction: International Series of Monographs in Experimental Psychology*; Elsevier, (2013) .
28. Berti, S., Vossel, G. and Gamer, M. (2017) The Orienting Response in Healthy Aging: Novelty P3 Indicates No General Decline but Reduced Efficacy for Fast Stimulation Rates. *Front. Psychol.*, **8**, 1780.
29. Wang, C.-A. and Munoz, D.P. (2015) A circuit for pupil orienting responses: implications for cognitive modulation of pupil size. *Curr. Opin. Neurobiol.*, **33**, 134–140.
30. Cohen, N.J. and Douglas, V.I. (1972) Characteristics of the orienting response in hyperactive and normal children. *Psychophysiology*, **9**, 238–245.
31. Harris, N.S., Courchesne, E., Townsend, J., Carper, R.A. and Lord, C. (1999) Neuroanatomic contributions to slowed orienting of attention in children with autism. *Brain Res. Cogn. Brain Res.*, **8**, 61–71.
32. Leitner, Y. (2014) The co-occurrence of autism and attention deficit hyperactivity disorder in children - what do we know? *Front. Hum. Neurosci.*, **8**, 268.
33. Demontis, D., Walters, R.K., Martin, J., Mattheisen, M., Als, T.D., Agerbo, E., Baldursson, G., Belliveau, R., Bybjerg-Grauholm, J., Bækvad-Hansen, M., *et al.* (2019) Discovery of the first genome-wide significant risk loci for attention deficit/hyperactivity disorder. *Nat. Genet.*, **51**, 63–75.
34. Kucewicz, M.T., Dolezal, J., Kremen, V., Berry, B.M., Miller, L.R., Magee, A.L., Fabian, V. and Worrell, G.A. (2018) Pupil size reflects successful encoding and recall of memory in humans. *Sci. Rep.*, **8**, 4949.
35. Tsukahara, J.S. and Engle, R.W. (2021) Is baseline pupil size related to cognitive ability? Yes (under proper lighting conditions). *Cognition*, **211**, 104643.
36. Aston-Jones, G. and Cohen, J.D. (2005) An integrative theory of locus coeruleus-norepinephrine function: adaptive gain and optimal performance. *Annu. Rev. Neurosci.*, **28**, 403–450.

37. Nieuwenhuis, S., De Geus, E.J. and Aston-Jones, G. (2011) The anatomical and functional relationship between the P3 and autonomic components of the orienting response. *Psychophysiology*, **48**, 162–175.
38. Cocker, K.D., Fielder, A.R., Moseley, M.J. and Edwards, A.D. (2005) Measurements of pupillary responses to light in term and preterm infants. *Neuroophthalmology*, **29**, 95–101.
39. Amendola, E., Zhan, Y., Mattucci, C., Castroflorio, E., Calcagno, E., Fuchs, C., Lonetti, G., Silingardi, D., Vyssotski, A.L., Farley, D., *et al.* (2014) Mapping pathological phenotypes in a mouse model of CDKL5 disorder. *PLoS One*, **9**, e91613.
40. Mattapallil, M.J., Wawrousek, E.F., Chan, C.-C., Zhao, H., Roychoudhury, J., Ferguson, T.A. and Caspi, R.R. (2012) The Rd8 mutation of the Crb1 gene is present in vendor lines of C57BL/6N mice and embryonic stem cells, and confounds ocular induced mutant phenotypes. *Invest. Ophthalmol. Vis. Sci.*, **53**, 2921–2927.
41. Silasi, G., Xiao, D., Vanni, M.P., Chen, A.C.N. and Murphy, T.H. (2016) Intact skull chronic windows for mesoscopic wide-field imaging in awake mice. *J. Neurosci. Methods*, **267**, 141–149.
42. Bishop, C.M. (2006) Pattern Recognition and Machine Learning. *Pattern Recognition and Machine Learning*; Springer, (2006) .
43. Platt, J. and Others (1999) Probabilistic outputs for support vector machines and comparisons to regularized likelihood methods. *Advances in large margin classifiers*, **10**, 61–74.
44. Rasmussen, C.E. and Williams, C.K.I. (2005) Gaussian Processes for Machine Learning. *Gaussian Processes for Machine Learning*; MIT Press, (2005) .
45. Hastie, T., Tibshirani, R. and Friedman, J. (2013) The Elements of Statistical Learning: Data Mining, Inference, and Prediction. *The Elements of Statistical Learning: Data Mining, Inference, and Prediction*; Springer Science & Business Media, (2013) .
46. Freund, Y. and Schapire, R.E. (1997) A Decision-Theoretic Generalization of On-Line Learning and an Application to Boosting. *Journal of Computer and System Sciences*, **55**, 119–139.
47. Hinton, G.E. (1989) Connectionist Learning Procedures. *Artificial Intelligence 1989*, **40**, 185–234.